DOI: 10.24425/118967

I. DZIOBA*, P. FURMANCZYK**#, S. LIPIEC*

DETERMINATION OF THE FRACTURE TOUGHNESS CHARACTERISTICS OF S355JR STEEL

The article presents the results of tests carried out on S355JR steel of ferrite-pearlite and ferrite-bainite microstructures. The strength properties and fracture toughness were determined. The critical value of fracture toughness was determined at the moment of crack initiation by measuring of the stretch zone width, and in the moment of reaching a subcritical crack growth of 0.2 mm. Determination of fracture toughness characteristics was carried out in accordance with the procedures of ISO and ASTM standards.

Keywords: S355JR steel, strength properties, fracture toughness, stretch zone width

1. Introduction

Low carbon steels of the ferritic matrix, including steel S355JR are commonly used to perform various kinds of engineering elements and constructions. Products manufactured in steel mills typically have a microstructure of ferrite-pearlite and ferrite-bainite-pearlite [1,2]. Elements made of these steels are often joined by various welding methods, which leads to the formation of ferritic-bainitic or bainitic types of microstructures in heat affected zones [3,4].

To evaluate the strength of the structural elements is necessary to know the characteristics of strength and fracture toughness of the material. While the level of conservative assessment depends on quality of the possessed characteristics of the material, regularity of selected research methods and accuracy of their implementation [5].

Procedure for determining the fracture toughness characteristics in the case of subcritical development of crack is quite complicated [6]. The development of subcritical crack in this case is not realized at one time, and is a process, that consists of several steps (Fig. 1). In the first step, as a result of the load applied, tip of the fatigue pre-crack becomes blunt and the banks of crack opened to the certain critical size δ_{TC}. In the next stage, which is considered to be the initiation moment, subcritical crack starts to propagate. The characteristics of fracture toughness, at this moment determined, are designated as J_i, δ_{TC} [7].

The ASTM standard suggests to determine the critical value of fracture toughness, J_{IC}, at the subcritical crack increment Δa = 0.2 mm. In the case of obtaining the fracture toughness critical value for materials with a high ductility additional difficulties arise, connected with the fact that the subcritical crack initiation begins firstly in the middle of the specimen thickness, and gradually extends to the sides. Also, in the middle part of the specimen, the increase of the subcritical crack is much larger than at the sides. Such process of subcritical crack growth is related with a reduction of the plane strain state part at the tip of the crack with increasing plastic properties of the material.

This article presents the results of research related to the appointment of the characteristics of fracture toughness of the S355JR steel of ferrite-pearlite and ferrite-bainite microstructures, significantly differing in the levels of strength and ductility.

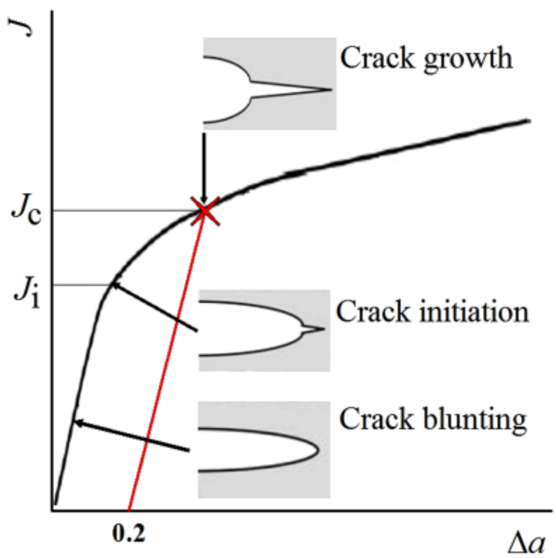

Fig. 1. Diagram of ductile sub-critical crack extension [8]

* DEPARTMENT OF MECHANICAL DESIGN, FACULTY OF MECHATRONICS AND MECHANICAL ENGINEERING,KIELCE UNIVERSITY OF TECHNOLOGY, 7 TYSIACLECIA P.P. AL., 25-314 KIELCE, POLAND
** DEPARTMENT OF METAL SCIENCE AND MANUFACTURING PROCESSES, FACULTY OF MECHATRONICS AND MECHANICAL ENGINEERING, KIELCE UNIVERSITY OF TECHNOLOGY, 7 TYSIACLECIA P.P. AL., 25-314, KIELCE, POLAND
# Corresponding author: pfurmanczyk@tu.kielce.pl

2. Material and methods

The analysis of fracture process was carried out on the specimens of low-alloy steel of middle strength S355JR, made according to the standard [8].

Semi-finished products with dimensions of 12.5×25×120 mm were subjected to the laboratory heat treatment, according to the scheme shown in Figure 2.

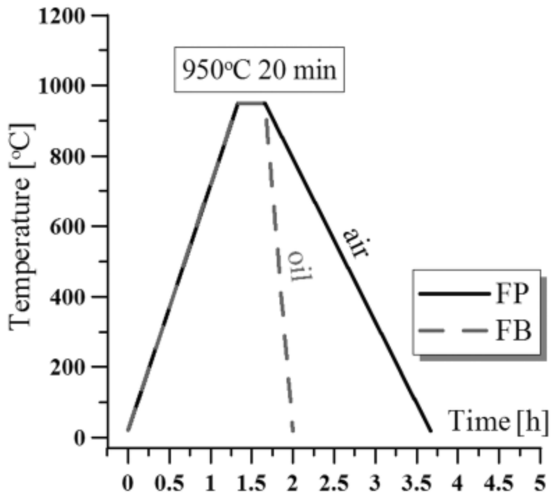

Fig. 2. The heat treatment regimes of S355JR steel

In a result of the heat treatment were obtained two types of microstructures: ferritic-pearlitic (FP) (Fig. 3a) and ferrite-bainite (FB) (Fig. 3b). S355JR steel strength characteristics with two types of microstructure were determined as a result of a uniaxial tensile test [9]. Tests were carried out on standard specimens with an initial diameter of 5 mm and the extensometer base of 25 mm.

The specimens were loaded until failure. Based on data obtained during the test, nominal value of stresses and strains until the necking on a specimen, were determined the true values of stresses and strains according to the relation:

$$\sigma_t = \sigma_n(1 + \varepsilon_n) \quad (1)$$

$$\varepsilon_t = \ln(1 + \varepsilon_n) \quad (2)$$

where:

ε_n – nominal strain,

σ_n – nominal stress.

In the Figure 4 are shown the stress-strain curves for nominal and true values of S355JR steel of ferrite-pearlite (black lines) and ferritic-bainitic (grey lines) microstructure. In Table 1 are placed the strength characteristics and hardness measurement results of tested types of S355JR steel. The nominal and true values, which according to lower yield strength, σ_{LYS}, upper yield strength, σ_{UYS}, and ultimate strength, σ_{UTS}, are listed. The values of Young's modulus, E, and material hardening exponent, *n*, from the Ramberg-Osgood equation obtained from true stress-strain dependences are presented also. All of these characteristics would used following during obtaining of the fracture toughness critical values.

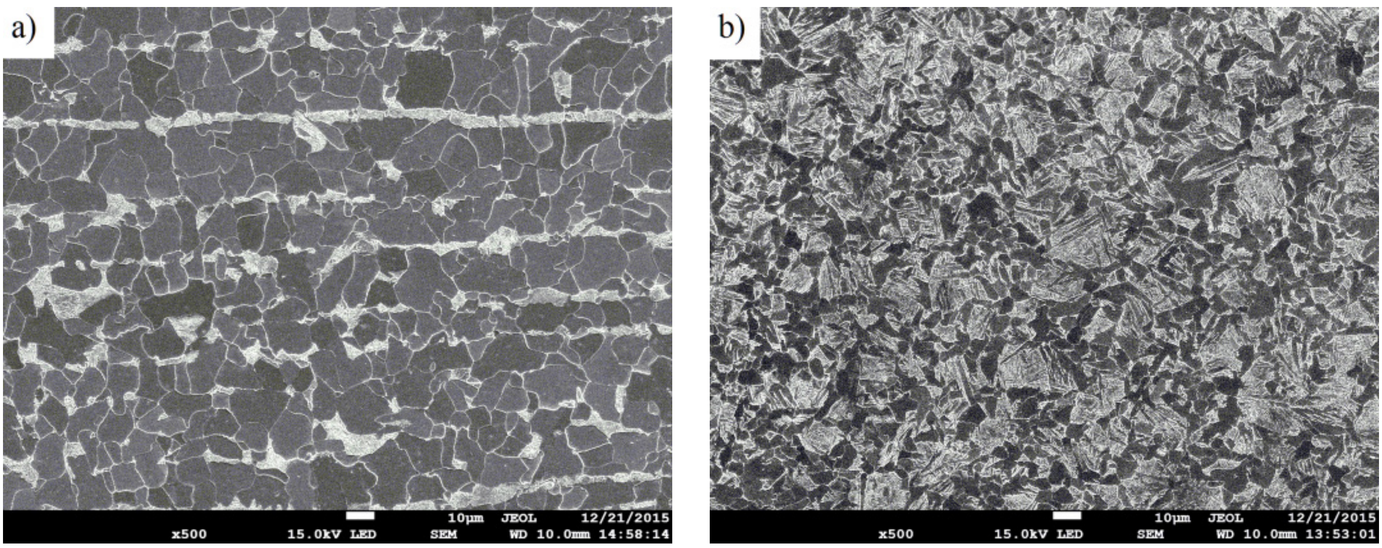

Fig. 3. Microstructure of the S355JR steel: a) ferritic-pearlitic, b) ferritic-bainitic

TABLE 1

The mechanical properties of S355JR steel of *FP* and *FB* microstructure types

Microstr. type	**σ_{YS}, MPa**				**$\sigma_{0.2}$, MPa**		**σ_{UTS}, MPa**		***E*, GPa**	***n***	**A_5, %**	***HV*10**
	σ_{LYS}	**σ_{UYS}**	**σ_{LYS}**	**σ_{UYS}**	**Nom.**	**True**	**Nom.**	**True**	**True**	**True**		
	Nom.		**True**									
FP	367	386	378	396	—	—	495	613	197	7.77	36	144
FB	—		—		463	466	679	771	206	8.25	24	194

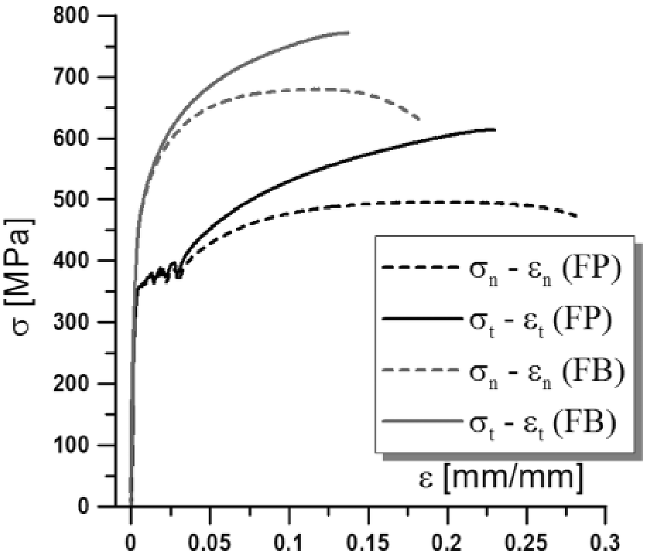

Fig. 4. The stress-strain curves of S355JR steel

3. The fracture toughness of S355JR steel according to ASTM standard

S355JR steel is a material with a middle strength level and high plasticity, therefore the critical value of fracture toughness was determined by the critical value of integral J, J_{IC}. The test for estimation of the critical value of fracture toughness was carried out using the technique of changing compliance. During the test on the testing machine UTS/Zwick (100 kN) recorded signals are: load (P), opening the crack mouths (δ_M) and the displacement of the point of load application (Δu_{ext}). Two types of specimens with single-edge-notched- bend (SENB) of S355JR steel with dimensions: $W = 24$ mm, $B = 12$ mm, $a_0/W \approx 0.55$ and with side grooves of 1mm depth along the crack propagation (denotation of FP, FB), and notched to a depth of 1 mm by lateral grooves along the plane of crack propagation, with side grooves (indicated as FP_{sg}, FB_{sg}) were tested. Because the tested steel is of highly plastic, so acceptance for testing variants of specimen with side notches was to create in the cross-section of the tested specimen the stress-strain state similar to the plane strain state.

In order to determine the characteristics of fracture toughness, the several different methods suggested in the standards were used. In the first approach determination of the critical value of J-integral conducted in accordance with ASTM [10]. Due to the high flexibility of the tested steel, during the execution of the procedure to determine the critical value of fracture toughness, according to the change of compliance methods were shown differences between the subcritical crack extension, Δa, obtained from calculation by this method, and the one received by using of the microscopy measurement of Δa, directly on the fracture surface of the specimen breakthrough. Taking into account the differences in these values, an adjustment was made to increase the subcritical crack length to the formula:

$$\Delta a_{i\_cor} = \Delta a_{i\_cal} \frac{\Delta a_{mes}}{\Delta a_{cal}} \tag{3}$$

where:

- Δa_{i_cal} – next i increments subcritical growth crack obtained during the calculations;
- Δa_{cal} – total increase in the crack growth obtained as a result of the nomination procedure for assessment of the critical value of fracture toughness;
- Δa_{mes} – total increase in growth crack obtained by measuring the fracture surfase of tested up specimen.

Determined critical value of the J-integral, J_{IC}, based on the increase in subcritical crack length obtained during the calculations and after the correction. Data marked FP, FB, FP_{sg}, FB_{sg} and FP_{cor}, FB_{cor}, FP_{sg_cor}, FB_{sg_cor} accordigly.

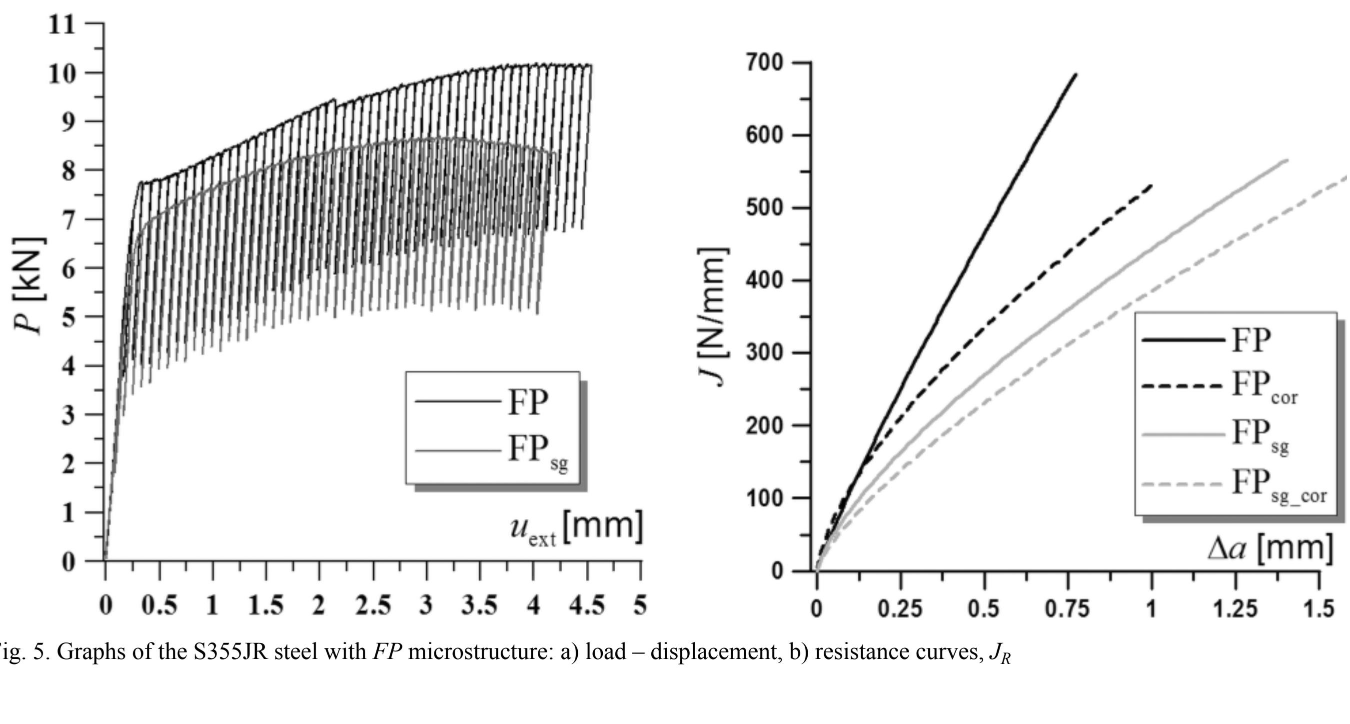

Fig. 5. Graphs of the S355JR steel with FP microstructure: a) load – displacement, b) resistance curves, J_R

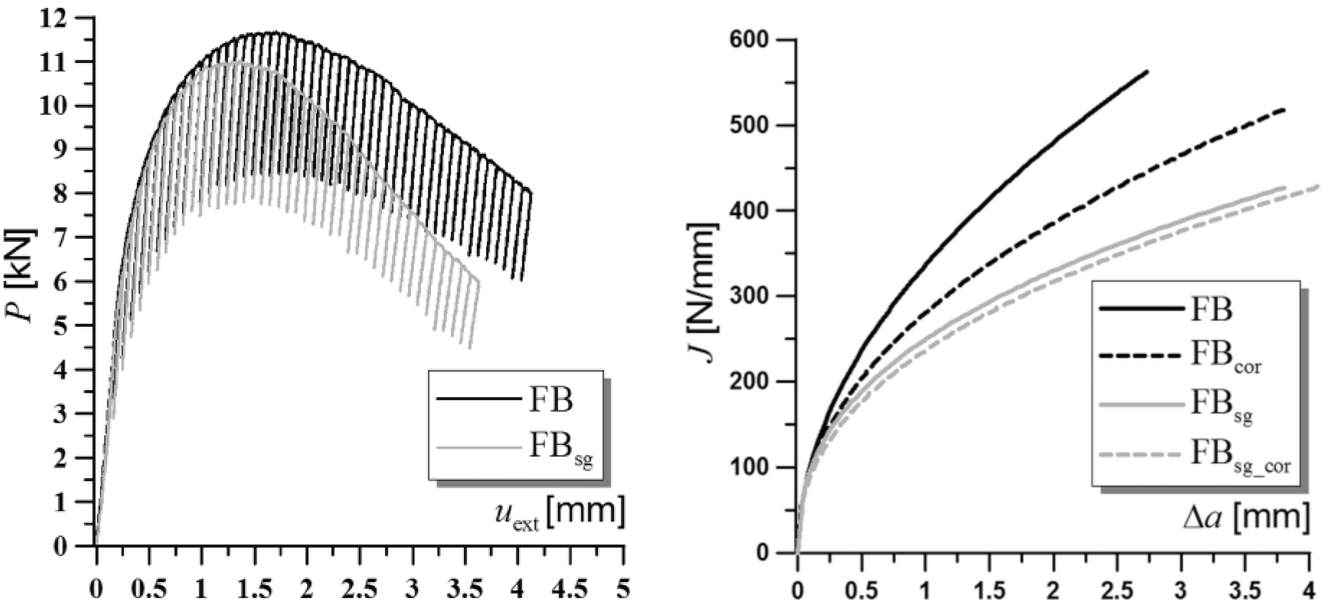

Fig. 6. Graphs of the S355JR steel with *FB* microstructure: a) load – displacement, b) resistance curves, J_R

4. The fracture toughness of S355JR steel at the moment of sub-critical crack initiation

As a result of blunting the fatigue pre-crack tip before initiation of the subcritical crack is formed a stretch zone. Some of the norms recommend calculation the critical value of the *J*-integral at the moment of initiation of the subcritical crack, J_i, on the basis of the determined width of stretch zone (*SZW* or Δa_{SZW}) [7,11,12]. On the fracture surface of the broken specimen, the stretch zone can be observed between the area of fatigue crack and the area of the subcritical crack extension (Fig. 7). It should be noted that the critical value of fracture toughness at the moment of initiation, J_i, is less than the critical value of *J*-integral, J_{IC}, that is particularly noticeable at ductile growth of the subcritical crack. This difference is a consequence from the fact that the critical value of the *J*-integral, J_{IC}, is determined for the average growth of the subcritical cracks, $\Delta a = 0.2$ mm, when the fracturing process occurred.

Measurements of the width of the stretch zone were made based on the recommendations published by the European standards ESIS [7], GKSS [11] and ISO-12135:2002 [12]. In accordance with the recommendation the width of stretch zone performed by using an electron scanning microscope. Determination of fracture toughness at the moment of initiation of cracking with measurements width of stretch zone was carried out in two stages. At the first stage, were made the pictures of the

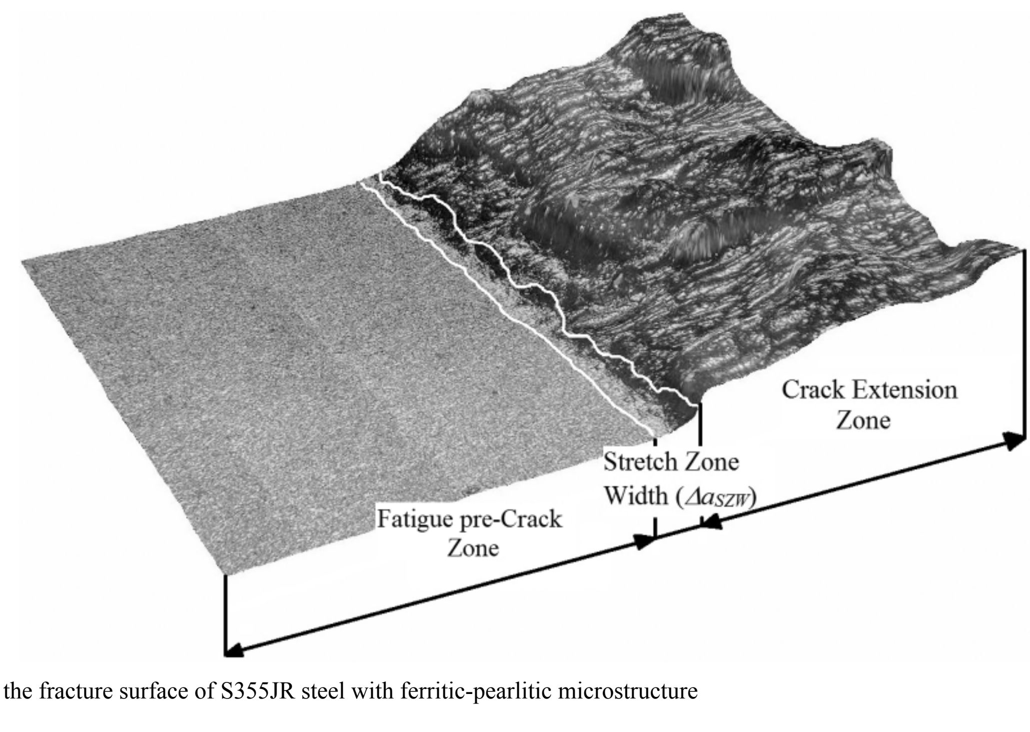

Fig. 7. Profile of the fracture surface of S355JR steel with ferritic-pearlitic microstructure

stretch zone with the help of scanning electron microscope JEOL 7100F field emission at a magnification of ×300 and a working distance of 25 mm. The measurement area of 1 mm in length is situated in the axis of the specimen breakthrough because of the dominance of plane strain state in this area.

The distance between the center points of the measurement areas was 300 μm, and the determinant of the breakthrough axis was a fatigue crack tip (Fig. 8). To determine the sampling points was used the microscope software, that allows to keep the constant coordinates of the nearest 0.001 mm. The width of the stretch zone, Δa_{SZW}, was obtained by measuring the surface area of the stretch zone of 3 measurement places. To determine Δa_{SZW} from the SEM pictures of surface area was used public program “Makroaufmassprogramm” [13].

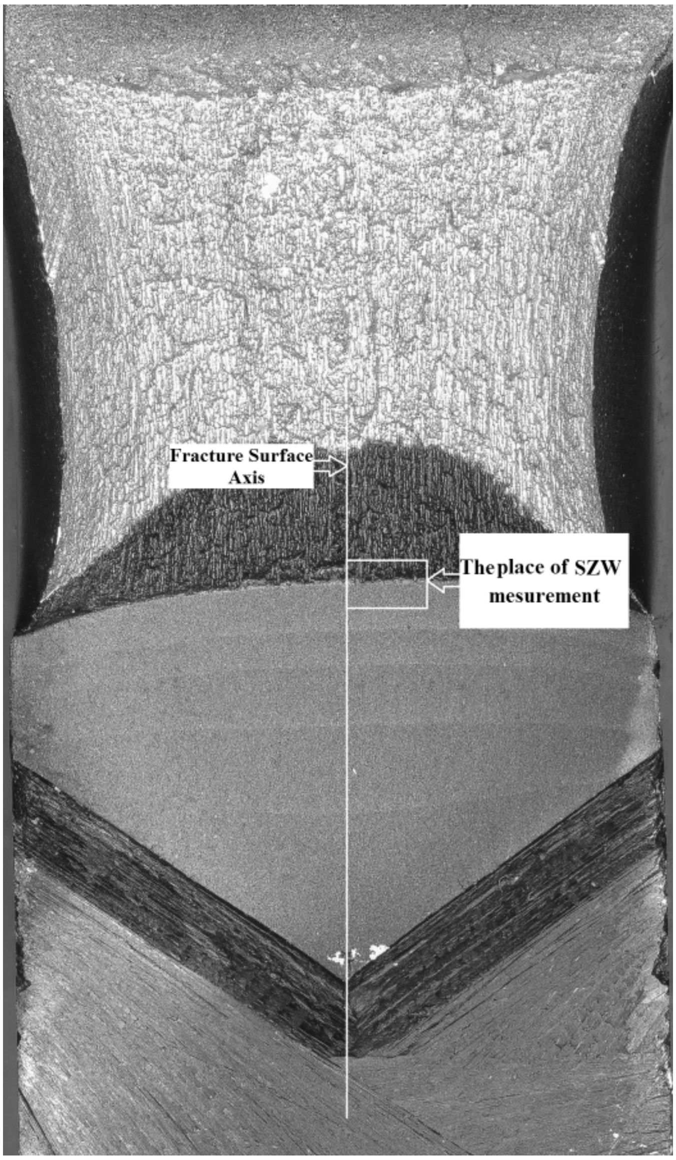

Fig. 8. Macro view of the fracture surface of S355JR steel with ferritic-pearlitic microstructure

The borders of stretch zone are not clear. It has of irregular waveform (Fig. 9a-d). This is caused by some problems precise determination of the start and end points during measurement of stretch zones width. Experience in the analysis of a fracture surfaces is required from the microscope operator performing this test. Determination of the width of the stretch zone based on an evaluation of the surface area allows to get more accurate value. Critical value of fracture toughness at the moment of initiation of subcritical crack propagation, J_i, calculated on the base of the average value of the *SZW*, $\Delta\bar{a}_{SZW}$. The calculations are based on the relation proposed by Shih for materials with high plasticity [14]:

$$J_i = \frac{2\sigma_Y}{d_n}\Delta\bar{a}_{SZW} \qquad (4)$$

where:

σ_Y – is equal $\sigma_Y = 0.5(\sigma_{YS} + \sigma_{UTS})$, σ_{YS} is a yield strength, σ_{UTS} is ultimate strength;

d_n – is a factor that depends on material hardening exponent, n, from the Ramberg-Osgood equation [14-16].

The values obtained during the calculation using the equation (4) with the average values of the *SZW* are summarized in Table 3.

5. Conclusions

In this study tried to compare the characteristics of strength and fracture toughness of S355JR steel with two different types of microstructure, obtained as a result of a laboratory heat treatment. S355JR steel with a ferritic-bainitic microstructure was characterized by higher level of strength and hardness, while the steel with a ferritic-pearlitic microstructure has higher plasticity and fracture toughness.

Due to the high level of plasticity of S355JR steel with ferrite-pearlite microstructure the condition of plain strain state was not provided on the SENB smooth specimens without side-grooves during determination of the critical value of fracture toughness according to the ASTM procedure. The condition of plain strain state in the plane of subcritical crack growth

TABLE 2

The critical values of the fracture toughness J_C, J_{IC}, extension of sub-critical crack Δa and required values of the critical specimens thickness B_C

Microstructure	J_C, J_{IC}, N/mm	Δa_{cal}, mm	Δa_{mes}, mm	B_C, mm
FP	—	0.71	1.13	—
FP_{cor}	364*	1.09		24.05
FP_{sg}	250*	1.16	1.47	16.52
FP_{sg_cor}	194*	1.44		12.82
FB	200	2.72	3.8	10.79
FB_{cor}	171	3.7		9.23
FB_{sg}	159	3.8	4.2	8.58
FB_{sg_cor}	146	4.2		7.88

* – for this data the requirement on specimen thickness, $B \geq B_C$, is not performed

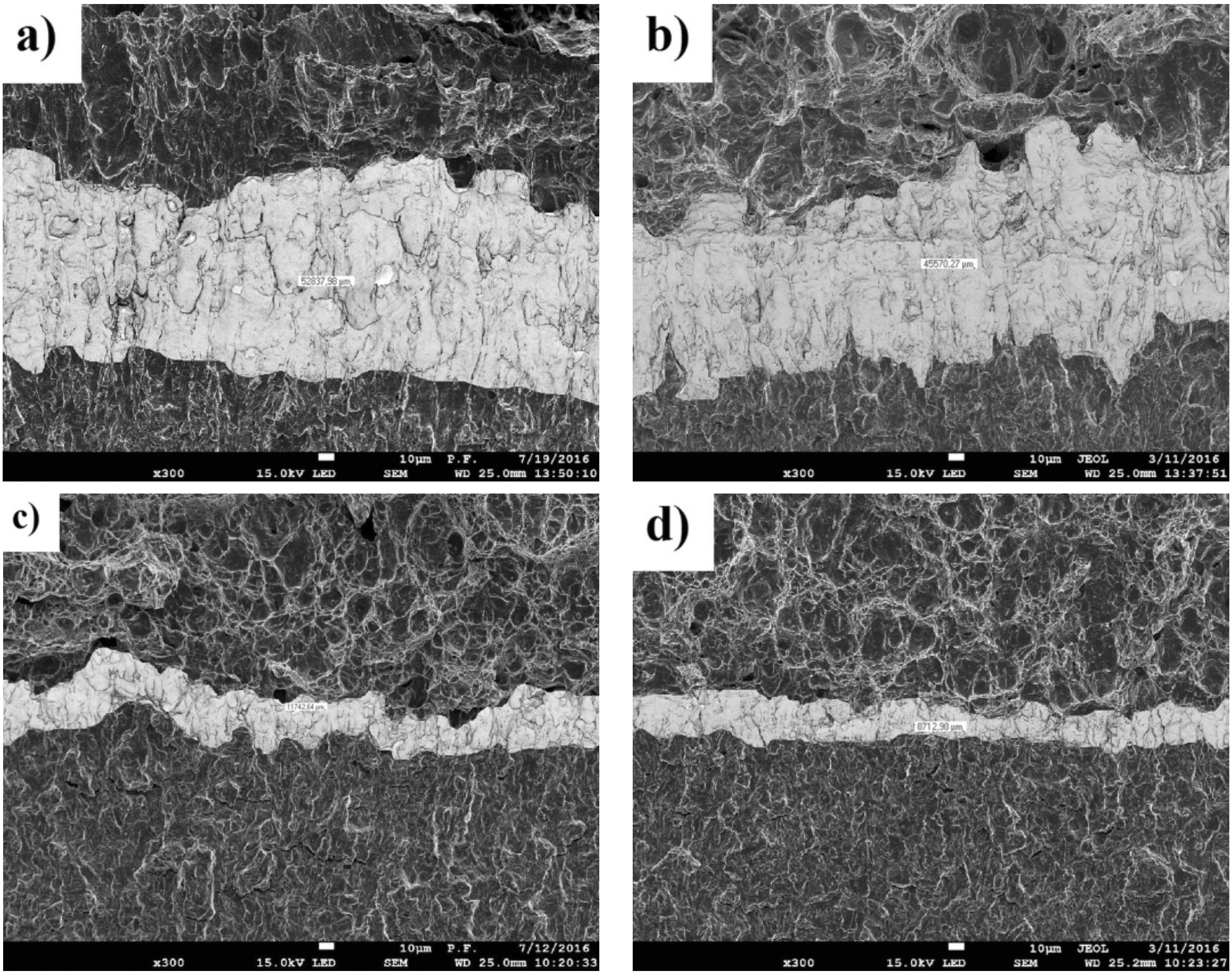

Fig. 9. SEM photographs with estimated *SZW* of S355JR steel: a) *FP*, b) FP_{sg}, c) *FB*, d) FB_{sg}.

was obtained on specimens with notches side-grooves. On the specimens with the side-grooves were obtained lower values of fracture toughness in comparison with smooth specimens (Table 2), namely for the specimens of ferritic-perlitic microstructure reduction of fracture toughness level is almost two-fold.

The fracture toughness level at the moment of subcritical crack initiation J_i is significantly lower, than the J_{IC} obtained according to the ASTM standard procedure for crack extension for Δa = 0.2 mm. Because at the determining values of J_i were included the width of the stretch zone only in the axis of the specimens, results obtained from smooth specimens and side grooved are similar to each other (Table 3). In the case if stretch zone width is determined over the entire width of the specimen, reducing of the average value of the area is observed, and accordingly the received characteristics of the fracture toughness are lower [17].

TABLE 3

Data of the *SZW* measurement and J_i calculation

Microstructure	Δa_{SZW}, **μm**	J_i, **N/mm**
FP	101.53	249.46
FP_{sg}	100.93	250.05
FB	24.44	59.34
FB_{sg}	24.93	60.60

Acknowledgements

The work was performed as part of research projects: 01.0.08.00/2.01.01.01.0008 MNSP.MKPK.16.001; 01.0.06.00/2.01.01.02.0020 MNSC.MKTK.16.004 and 01.0.08.00/2.01.01.02.0021 MNSC.MKPK.16.002

REFERENCES

[1] J. Zhao, J.H. Lee, Y.W. Kim, Z. Jiang, Ch.S. Lee, Materials Science and Engineering **559,** 427-435 (2015).

[2] B. Ligaj, The influence of selected loading programmers generated from the correlation table on fatigue life of 18G2A steel, Maintenance Problems **3**, 129-246 (2007).

[3] M. Sokolov, A. Salminen, M. Kuznetsov, I. Tsibulskiy, Materials and Design **32**, 5127-5131 (2011).

[4] I. Dzioba, A. Skrzypczyk, Welding Technology Review **78**, 32-35 (2006).

[5] M. Kocak, S. Webster, J.J. Janosch, R.A. Ainsworth, R. Koerc, FITNET Fracture-Fatigue-Creep-Corrosion, 2008.

[6] T.L. Anderson, Fracture Mechanics: Fundamentals and Applications, 2008.

[7] ESIS Procedure for Determining the Fracture Behaviour of Materials. ESIS P2-92 (1992). Appendix 4. s. A4.1-A4.6

[8] PN-EN 10025-2: 2007, Hot Rolled Products Of Structural Steels. Part 2. Technical Delivery Conditions for Non-Alloy Structural Steels (2007).

[9] ASTM E8, Standard test method for tension testing of metallic materials, ASTM International West Conshohocken, PA (2003).

[10] ASTM E1820-09, Standard Test Method for Measurement of Fracture Toughness, ASTM International West Conshohocken, PA (2009).

[11] K.H. Schwalbe, J.D. Landes, J. Heerens, Classical Fracture Mechanics Methods, GKSS 2007/14.2007.

[12] ISO 12135:2002 Metallic materials – Unified method of test for the determination of quasistatic fracture toughness (2002).

[13] http:/reudig.de/tmp/messprogramm.htm, accessed: 28.06.2017.

[14] A. Neimitz, Mechanika Pękania (in Polish) Warszawa PWN 1999.

[15] H. Kobayashi, H. Nakamura, H. Nakazawa, Evaluation of Blunting Line and Elastic-Plastic Fracture Toughness, ASTM STP **803**, 420-438 (1983).

[16] W. L. Guo, Elastoplastic three dimensional crack border field – III. Fracture parameters, Engineering Fracture Mechanics **51**, 51-57 (1995).

[17] I. Dzioba, P. Furmańczyk, Wyznaczanie krytycznych wartości odporności na pękanie *Ji* na podstawie pomiaru szerokości strefy stępienia (in Polish), Wybrane problemy w mechatronice i inżynierii materiałowej, 110-123 (2016).